Universiteit Antwerpen

This item is the archived peer-reviewed author-version of:

Small-moment paramagnetism and extensive twinning in the topochemically reduced phase $Sr_2ReLiO_{5.5}$

Reference:

Hasanli Nijat, Gauquelin Nicolas, Verbeeck Johan, Hadermann Joke, Hayw ard Michael A..- Small-moment paramagnetism and extensive tw inning in the topochemically reduced phase $Sr_2ReLiO_{5.5}$

Journal of the Chemical Society: Dalton transactions / Chemical Society [London] - ISSN 1477-9226 - 47:44(2018), p. 15783-15790

Full text (Publisher's DOI): https://doi.org/10.1039/C8DT03463J

To cite this reference: https://hdl.handle.net/10067/1557710151162165141

uantwerpen.be

Institutional repository IRUA

Small-moment paramagnetism and extensive twinning in the topochemically reduced phase $Sr_2ReLiO_{5.5}$

Nijat Hasanli,[a] Nicolas Gauquelin,[b,c] Johan Verbeeck,[b] Joke Hadermann [b] and Michael A Hayward [a]*

Reaction of the cation-ordered double perovskite Sr_2ReLiO_6 with dilute hydrogen at 475 °C leads to the topochemical deintercalation of oxide ions from the host lattice and the formation of a phase of composition $Sr_2ReLiO_{5.5}$, as confirmed by thermogravimetric and EELS data. A combination of neutron and electron diffraction data reveals the reduction process converts the –Sr_2O_2–$ReLiO_4$–Sr_2O_2–$ReLiO_4$– stacking sequence of the parent phase into a –Sr_2O_2–$ReLiO_3$–Sr_2O_2–$ReLiO_4$–, partially anion-vacancy ordered sequence. Furthermore a combination of electron diffraction and imaging reveals $Sr_2ReLiO_{5.5}$ exhibits extensive twinning – a feature which can be attributed to the large, anisotropic volume expansion of the material on reduction. Magnetisation data reveal a strongly reduced moment of μ_{eff} = 0.505 μ_B for the d^1 Re^{6+} centres in the phase, suggesting there remains a large orbital component to the magnetism of the rhenium centres, despite their location in low symmetry coordination environments.

Introduction

There has been much interest in complex oxides containing 5*d* transition metals because these phases can have physical and chemical properties which are qualitatively different from the more widely studied 3*d* systems.[1] The principal differences between 5*d* and 3*d* transition metal oxides can be attributed to the greater radial extension of the 5*d* orbitals which, when they are incorporated into oxide lattices, leads to the formation of broad electronic bands with only modest electron-electron correlation. Furthermore 5*d* metals experience much stronger spin orbit coupling (SOC) than 3*d* systems, so as a result the on-site coulombic repulsions (U), crystal field effects (Δ) and SOC interactions (λ) can be of comparable magnitude. This equivalence of energy scales can lead to unexpected behaviour, such as the antiferromagnetic insulating ground state of Sr_2IrO_4,[2] which can be attributed to strong SOC dividing the broad t_{2g}^5 band (derived from the Ir 5*d* orbitals) into a filled quartet $J = {}^3/_2$ band and a half-filled doublet $J = ½$ band, the latter of which is sufficiently narrow that a Mott gap can be opened by small coulombic repulsions (U).

A further feature arising from the similarity of the energy scales of U, Δ and λ is that small changes to any one of these interactions can lead to significant changes to the electronic and magnetic behaviour of 5*d* oxides systems. For example the influence of SOC depends on the degree to which the d_{xy}, d_{xz} and d_{yz} orbitals are energetically degenerate, which in turn depends on the local symmetry at the metal centre. As a result any changes in crystal symmetry which arise as a function of temperature, composition or due to electronic instabilities (i.e. a Jahn-Teller distortion) can modify the influence of SOC and thus change the magnetic and electronic behaviour of phases in a complex manner. These effects have been invoked to explain experimental observations such as the differing magnetic behaviour of Ba_2AReO_6 and Sr_2AReO_6 (A = Ca^{2+}, Mg^{2+}) phases,[3] the apparent observation of J_{eff} ≠ 0 $Ir^{5+}O_6$ centres,[4] [5] and the ferromagnetism of Ba_2NaOsO_6 [6, 7] and they allude to the rich variety of physical behaviour possible in 5*d* transition-metal oxides.

The major chemical differences between the heavy and light transition metals can also be attributed to the greater radial extent of the 5*d* orbitals, which in combination with the 2 radial nodes possessed by this orbital set (compared to zero radial nodes for the 3*d* orbitals) lead to a much greater stabilization of high oxidation states.[8] As a result many 5*d* transition metals are most commonly found in their diamagnetic (d^0) group oxidation states when located in oxide lattices, with the preparation of phases containing *5d* metals in lower oxidation states presenting a significant synthetic challenge, especially for elements early in the transition series.

Double perovskite oxides containing d^1 Re^{6+} or d^2 Re^{5+} centres exhibit interesting physical properties, such as the apparent spin-singlet state in La_2LiReO_6 or the half-metallic ferromagnetism of Sr_2FeReO_6.[9, 10] However these phases require elaborate and precise synthesis procedures to help stabilize the lower oxidation states of rhenium with respect to the Re^{7+} 'group' oxidation state. Topochemical reduction, via anion deintercalation offers an alternate route to access the lower oxidation states of 5*d* transition metals in oxide lattices.[11] This approach can be particularly advantageous, because reactions of this type operate under conditions in which reaction products are selected under kinetic control,[11] so the relatively poor thermodynamic stability of the lower oxidation states of the 5*d* metals is less of an obstruction to their preparation. Here we describe the topochemical reduction of the Re^{7+} double perovskite phase, Sr_2ReLiO_6,[12] to an Re^{6+} phase $Sr_2ReLiO_{5.5}$, which exhibits an extremely small magnetic moment suggesting the rhenium centres experience strong spin-orbit coupling despite residing in low-symmetry environments.

Experimental

Synthesis. Samples of Sr_2ReLiO_6 were prepared via a high-temperature ceramic route. A 2:1:1.25 molar ratio of $SrCO_3$ (99.994%) : Re metal (99.99%): Li_2CO_3 (99.998%) was ground together in an agate pestle and mortar and then heated in air at 900°C for 12 h to decompose the carbonates. The resulting material was reground, pressed into 13mm pellets and reheated in air at 900°C for one period 24 h. The resulting material was a single phase, confirmed by X-ray powder diffraction with lattice parameters in good agreement with literature values.[12] Samples of Sr_2ReLiO_6 were reduced by heating under a flow of 5% H_2 in N_2 as described below.

Characterisation. High-resolution synchrotron X-ray powder diffraction data were collected using instrument I11 at the Diamond Light Source Ltd. Diffraction patterns were collected using Si-calibrated X-rays with an approximate wavelength 0.825 Å, from samples sealed in 0.3 mm diameter borosilicate glass capillaries using the PSD detector. Neutron powder diffraction data were collected using the GEM diffractometer at ISIS from samples contained in cylindrical vanadium cans. Rietveld profile refinements were performed using the GSAS suite of programs.[13] Magnetization data were collected using a Quantum Design MPMS SQUID magnetometer. Thermogravimetric measurements were performed by heating powder samples at a rate of 5 °C min^{-1} under an oxygen atmosphere, using a Mettler-Toledo MX1 thermogravimetric microbalance. Scanning transmission electron microscopy electron energy loss spectroscopy (STEM-EELS) was performed on a Titan 80-300 microscope equipped with an aberration corrector for the probe forming lens and an electron monochromator yielding an energy resolution of 100meV with a Gatan Quantum spectrometer. This setup was used at 80kV acceleration voltage with an exposure time of 0.2ms/frame integrated for 5s and a dispersion of 0.05eV/pixel to collect the spectrum at the Re $O_{2,3}$ edge (35eV). Electron diffraction patterns were taken on Philips CM20 and FEI Tecnai microscopes, dark field images were obtained on the Tecnai microscope. Samples for all TEM techniques were prepared in a glove box filled with inert argon by crushing the powder and dispersing it in ethanol. A few drops of this solution were deposited on a copper grid covered with a holey carbon film. The samples were exposed to air for a few minutes at insertion into the microscope.

Results

Chemical and crystallographic characterisation. Powder samples of Sr_2ReLiO_6 were heated at 475 °C under a flow of 5% H_2 in N_2 for 4 periods of 4 h. X-ray powder diffraction data collected between heating periods showed a change in lattice parameters (expansion in *a* and *c*) consistent with the topochemical deintercalation of oxygen from the material. No further changes were observed in the diffraction data collected after the third heating period. Thermogravimetric data shown in Figure 1, collected during the reoxidation of Sr_2ReLiO_{6-x} back to Sr_2ReLiO_6 (as confirmed by X-ray powder diffraction), indicated that the composition of the reduced phase was $Sr_2ReLiO_{5.5}$.

Figure 2 shows the EELS spectra of the Re $O_{2,3}$ edge of $Sr_2ReLiO_{5.5}$ (magenta curve) compared with La_2ReLiO_6 (Re^{5+}),[9] Sr_2ReCoO_6 (Re^{6+})[14] and Sr_2ReLiO_6 (Re^{7+}).[12] For the Sr containing compounds, it was not possible to use the sharp Re $M_{4,5}$ edge at 1883eV due to the strong overlap with the Sr $L_{2,3}$ edge at 1940eV, therefore the Re $O_{2,3}$ edge was used. This edge, to our knowledge, has never been measured for different valences of Re and no reference data is available in literature. Therefore, the above mentioned compounds were measured, which allowed us to conclude, by visual comparison of the shape of the Re $O_{2,3}$ edge that the Re oxidation state in $Sr_2ReLiO_{5.5}$ appears to be a mixture of Re^{6+} and Re^{5+} with Re^{6+} being the majority. The discrepancy of the spectrum for the $Sr_2ReLiO_{5.5}$ compound with the Re^{6+} reference is due to the absence of the Li K edge at 55 eV for Sr_2ReCoO_6. Nonetheless, a linear least squares fitting using the EELSModel software [15] yields a ratio of 80 ± 5 % Re^{6+} in $Sr_2ReLiO_{5.5}$.

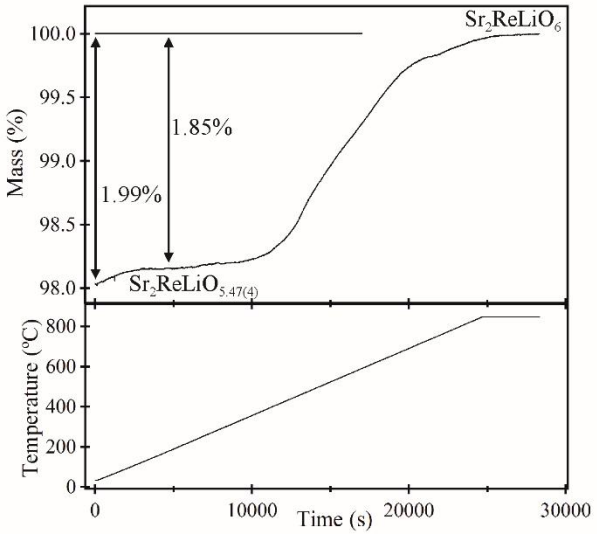

Figure 1. Thermogravimetric data collected during the reoxidation of $Sr_2ReLiO_{5.47(4)}$ to Sr_2ReLiO_6.

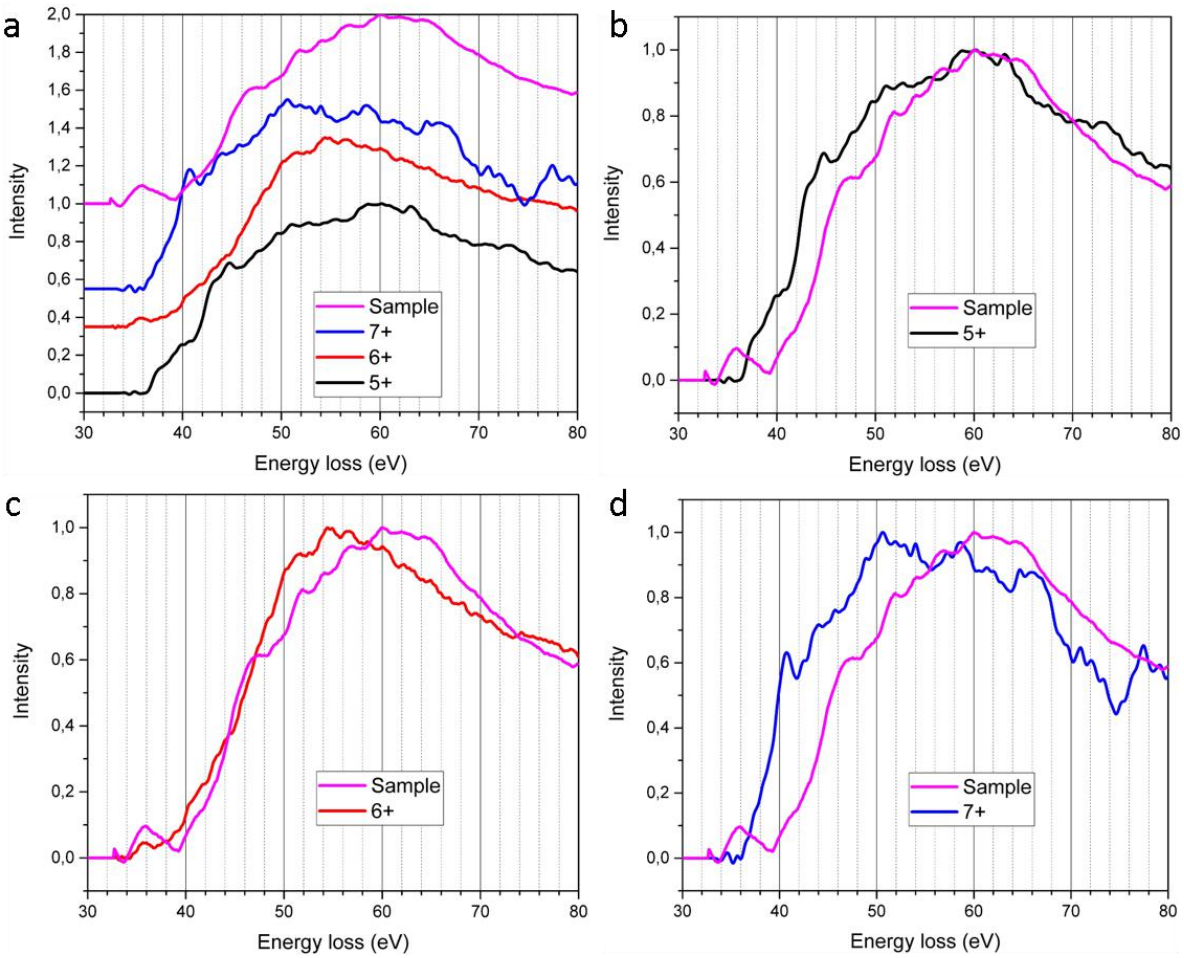

Figure 2. a) EELS measurement of the Re $O_{2,3}$ edge of $Sr_2ReLiO_{5.5}$ (Sample) compared with La_2ReLiO_6 (Re^{5+}), Sr_2ReCoO_6 (Re^{6+}) and Sr_2ReLiO^6 (Re^{7+}). For better visualisation the reference spectra for Re^{5+}, Re^{6+} and Re^{7+} were compared separately to the Sample spectrum in panels b, c and d.

Synchrotron X-ray and neutron powder diffraction data collected from $Sr_2ReLiO_{5.5}$ could be indexed using a primitive tetragonal unit cell (a = 5.521 Å, c = 8.114 Å). Thus a primitive tetragonal structural model (space group $P4/m$) was constructed, based on the body-centred tetragonal structure of Sr_2ReLiO_6,[12] and refined against the neutron diffraction data. Refinement of the oxide ion occupancies in the model led to a dramatic improvement in the fit to the data, with the best fit achieved when the oxygen vacancies were located in the 'equatorial' anion sites in alternate layers, such that the overall structure could be described by the stacking sequence: –Sr_2O_2–$ReLiO_3$–Sr_2O_2–$ReLiO_4$–.

Close inspection of the fit to the data using this tetragonal model revealed that the intensities of a number of diffraction peaks were not accounted for satisfactorily, as shown in Figure 3. To investigate if these intensity mismatches were due to anion-vacancy order leading to a geometrically expanded crystallographic unit cell, an electron microscopy study was performed.

A series of electron diffraction patterns were taken from several crystals, rotating the crystal to many different zones. All obtained patterns could be indexed using the primitive tetragonal cell obtained from the X-ray and neutron diffraction data, showing that the intensity mismatches are not due to a supercell. However, there was a high amount of twinning in all crystals. Representative patterns along some main zones are shown in Figure 4. The [1 $\bar{1}$ 0] pattern (Figure 4c) shows that the twinning occurs on the (112) plane, and involves a rotation of 90° around the [1 $\bar{1}$ 0] direction. This is schematically shown in Figure 4d. The same twin law also generates the combination [001]/[110] shown in Figure 4b. The twinning occurs on a fine scale, as visible in Figure 4e, showing a dark field image using only the 201 reflection (the approximate size of the aperture is indicated by a white circle), in zone [1 $\bar{1}$ 2] twinned with [2 $\bar{2}$ 1]. Unfortunately, in the main zones the reflections were too close together to select individual reflections with the available apertures. The twin domain sizes varied from crystal to crystal but were on average between 50-200 nm.

Given the absence of evidence for an expanded unit cell, the symmetry of the structural model was lowered from

tetragonal (*P*4/*m*) to orthorhombic (*Pmmm*) in an attempt to better fit the bulk diffraction data. It should be noted that there is no direct evidence for a lowering of crystal symmetry from the diffraction data (there are no split peaks or

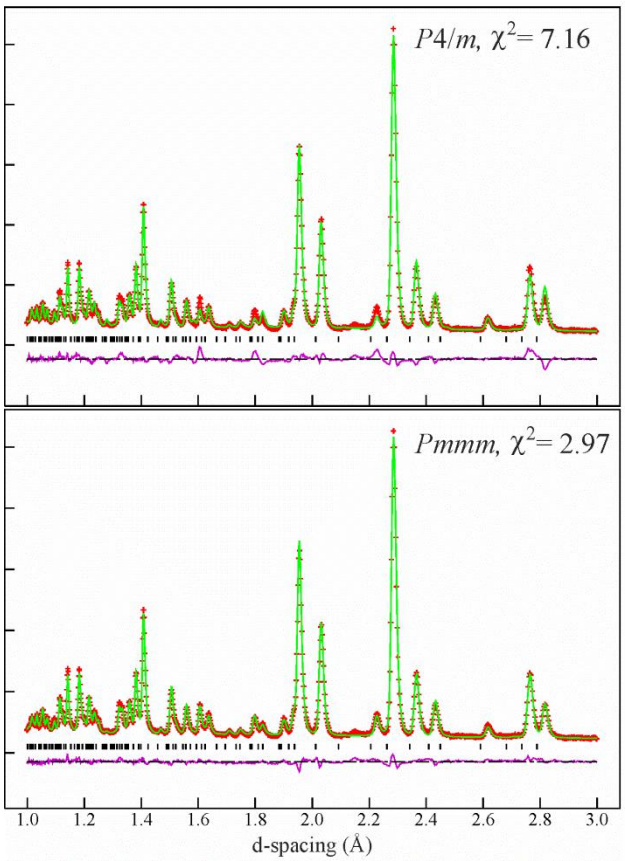

Figure 3. Observed calculated and difference plots from the refinement of tetragonal (top) and orthorhombic models (bottom) against neutron powder diffraction data collected from $Sr_2ReLiO_{5.5}$ at 300 K.

shouldering of peaks) however a lowering of the symmetry to orthorhombic led to an improvement in both the visual (Figure 3) and numerical fit to the data (χ^2 = 3.78) indicating that while the lattice parameters of $Sr_2ReLiO_{5.5}$are metrically tetragonal, the structure has orthorhombic symmetry. It was observed that the displacement parameters of the oxide ions were significantly larger than those of the cations, so all the anion displacements were changed to an anisotropic description. Refinement of these parameters led to the partially occupied anion site at position (*x*, *y*, ½) being described by a displacement ellipsoid which was highly elongated in a direction perpendicular to the Re-O-Li bond vector. This suggested a disordered rotation of the ReO_x and LiO_x polyhedra around the *z*-axis, therefore this anion site was split into two separate (*x*, *y*, ½) sites with half the occupancy of the original site, with the new sites described using isotropic displacement parameters. This model converged smoothly to give a good statistical fit (χ^2 = 2.97). The occupancies of all the anion sites were allowed to vary in the final refinement cycles, however the occupancies of sites O(1), O(2) and O(3) refined to unity within error, so were set at this value, and the occupancy of the O(4) and O(5) sites was constrained to maintain the composition determined by thermogravimetric analysis. A full description of the refined structure of $Sr_2ReLiO_{5.5}$ is given in Table 1, with selected bond lengths in

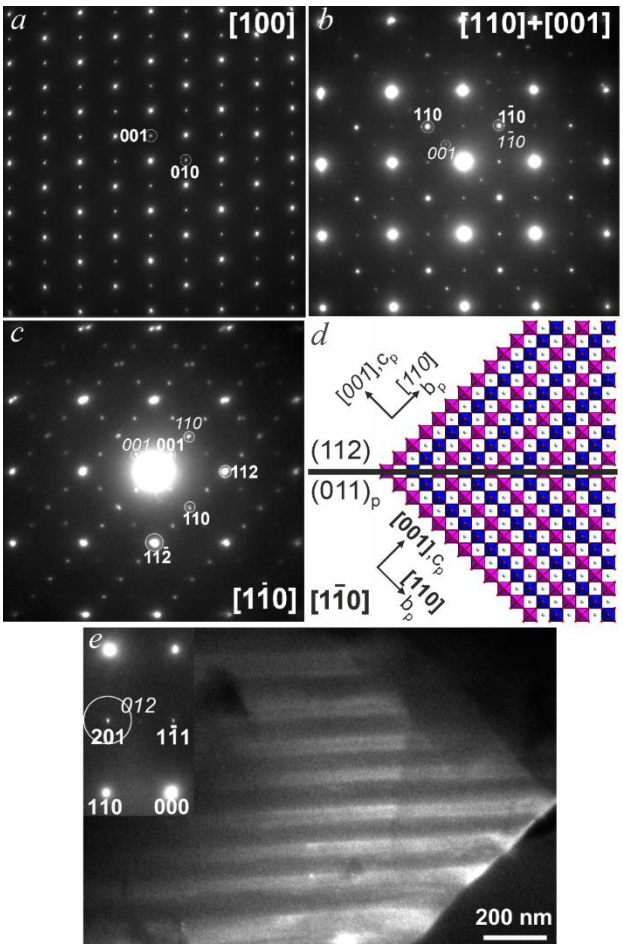

Figure 4. Electron diffraction patterns (a-c) and dark field TEM image (e) showing extensive twinning of $Sr_2ReLiO_{5.5}$ particles. Indices of the different twin components are given in bold versus italic. The schematic representation (d) visualizes the twins as seen along the [1 $\bar{1}$ 0] zone as in (c), blue and purple layers represent stoichiometric $ReLiO_4$ and reduced $ReLiO_3$ layers respectively. Indices with subscript 'p' indicate the lattice vectors of the 'single perovskite' lattice. Light and dark bands in (e) indicate domains related by 90° rotation around the [1 $\bar{1}$ 0] axis, imaged by selecting only the 201 reflection in a [1 $\bar{1}$ 2]/[2$\bar{2}$1] electron diffraction pattern (inset).

Table 2. Plots of the observed and calculated data are shown in Figure 3.

Magnetic and physical characterisation. Zero-field cooled (ZFC) and field cooled (FC) magnetisation data collected from $Sr_2ReLiO_{5.5}$ in an applied field of 1000 Oe are shown in Figure 5. The ZFC and FC are exactly coincident at all temperatures except 5K, where there is a very weak divergence. The data can be fit by the Curie-Weiss law (χ = C/(T-θ) + K) in the temperature range 20 < T/K < 300 to yield values of C = 0.0319(3) cm^3 K mol^{-1}, θ = -8.6(4) K and K = 2.38(1) × 10^{-4} cm^3 K mol^{-1}. The observed Curie constant is only 8.5 % of the value expected for a spin-only, S = ½ system, and corresponds to an effective rhenium moment of μ_{eff} = 0.505 μ_B. It

should also be noted that the temperature independent moment (2.38(1) × 10^{-4} cm^3 K mol^{-1}) corresponds to ~70% of the measured magnetisation at 300 K. The data were fitted over a number of different temperature intervals to test the robustness of the fit to the Curie-Weiss law. It was observed that the fitting range had no influence over the values of the parameters extracted, which appear independent of the temperature range fitted.

Deviation from the Curie-Weiss law at temperatures below T ~ 20 K could indicate the onset of magnetic order. However neutron powder diffraction data collected at 2 K show no additional features compared to the corresponding data collected at 300 K and can be fit to good statistical agreement by the crystallographic model refined at 300 K.

Table 1. Parameters from the structural refinement of $Sr_2ReLiO_{5.5}$ against neutron powder diffraction data collected at 298 K.

Atom	x	y	z	Fraction	U_{iso} (Å^2)
Sr(1)	½	0	0.2298(4)	1	0.0117(3)
Sr(2)	0	½	0.2232(4)	1	0.0117(3)
Re(1)	0	0	0	1	0.0059(1)
Re(2)	½	½	½	1	0.0059(1)
Li(1)	0.553(2)	½	0	0.5	0.0136(14)
Li(2)	0	0	½	1	0.0136(14)
O(1)	0.2514(4)	0.2291(3)	0	1	
O(2)	½	½	0.2725(2)	1	
O(3)	0	0	0.2414(2)	1	
O(4)	0.2955(9)	0.2415(9)	½	0.376(2)	0.0242(8)
O(5)	0.1795(9)	0.3875(9)	½	0.374(2)	0.0242(8)
Arom	U_{11}	U_{22}	U_{33}	U_{12}	
O(1)	0.0061(3)	0.0090(3)	0.0196(6)	-0.0063(2)	
O(2)	0.0191(4)	0.0183(4)	0.0109(7)	-	
O(3)	0.0191(4)	0.0183(4)	0.0109(7)	-	
$Sr_2ReLiO_{5.5}$ – Space group *Pmmm* (#47) Formula mass = 456.37, Z = 2 *a* = 5.5207(5) Å, *b* = 5.5216(5) Å, *c* = 8.1144(7)					
Radiation source: Tine-of-flight neutrons (GEM, ISIS) Temperature: 298 K χ^2 = 2.978; *wRp*= 4.51 %; *Rp* = 4.18 %.					

Table 2. Selected bond lengths from the refined structure of $Sr_2ReLiO_{5.5}$

Cation	Anion	length (Å)
Re(1)	O(1)	1.878(2)
	O(3)	1.959(2)
Re(2)	O(2)	1.846(2)
	O(4)	1.820(5)
	O(4)	1.875(5)
Li(1)	O(1)	1.854(7)
	O(1)	2.238(8)
	O(2)	2.230(2)
Li(2)	O(3)	2.098(2)
	O(4)	2.107(5)
	O(5)	2.358(5)
Sr(1)	O(1)	2.638(3)
	O(2)	2.782(1)
	O(3)	2.762(1)
	O(4)	2.804(4)
	O(5)	3.538(4)
Sr(2)	O(1)	2.728(3)
	O(2)	2.789(1)
	O(3)	2.765(1)
	O(4)	3.121(4)
	O(5)	2.532(4)

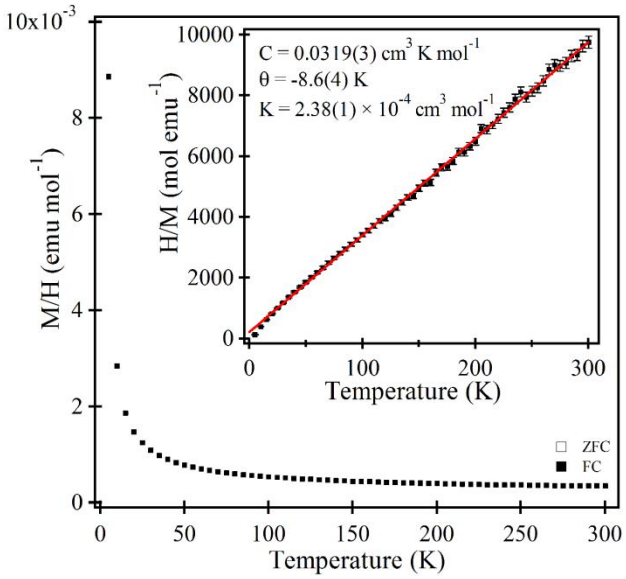

Figure 5. Zero-field cooled and field cooled magnetisation data collected from $Sr_2ReLiO_{5.5}$ in an applied field of 1000 Oe. Inset show fit to Cure-Weiss law in the temperature range 50 < T/ K 300.

Discussion

The topochemical reduction of Sr_2ReLiO_6 to the Re^{6+} phase $Sr_2ReLiO_{5.5}$ results in a 5.2% increase in the volume of the material. This volume increase occurs in a highly anisotropic manner, with only a 0.3% increase of the *a* and *b* lattice parameters, but a 4.6% increase in *c*. As a result the 'tetragonality' of the phase, defined as $c/(\sqrt{2}\times a)$ changes from 0.996 for Sr_2ReLiO_6 to 1.039 for $Sr_2ReLiO_{5.5}$. The extensive crystallographic twinning observed in $Sr_2ReLiO_{5.5}$ samples can be attributed to this highly anisotropic expansion – rotation by 90° around the [110] axis realigns the largest lattice expansion along the three principal Cartesian axes of the underlying perovskite framework to make the expansion isotropic when integrated over lengths of the order of ~1μm, thus reducing inter-particle strain. This division of particles into small domains is consistent with the apparent mismatch between the orthorhombic crystal symmetry of the phase and the metrically tetragonal lattice parameters of the

material and the lack of long-range anion-vacancy order in the material described below.

It has been noted previously that oxides containing the heavier 4*d* and 5*d* transition-metals are hard to reduce topochemically as they tend to be kinetically unstable with respect to complete reduction to yield the 4*d*/5*d* element. For example $SrRuO_3$ decomposes to form SrO + Ru under conditions where $SrFeO_3$ is topochemically reduced to $SrFeO_2$.[16] Likewise Sr_2IrO_4 is reduced to SrO + Ir under conditions where $LaSrCoO_4$ is reduced to $LaSrCoO_{3.38}$.[17] Typically 3*d* transition metals need to be introduced into materials to help stabilize reduced lattice containing the heavier 4*d*/5*d* metals. For example the introduction of iron can help to stabilize Ru^{2+} and Ir^{2+} in $SrFe_{0.5}Ru_{0.5}O_2$ and Sr_2FeIrO_4 respectively.[16] It is therefore

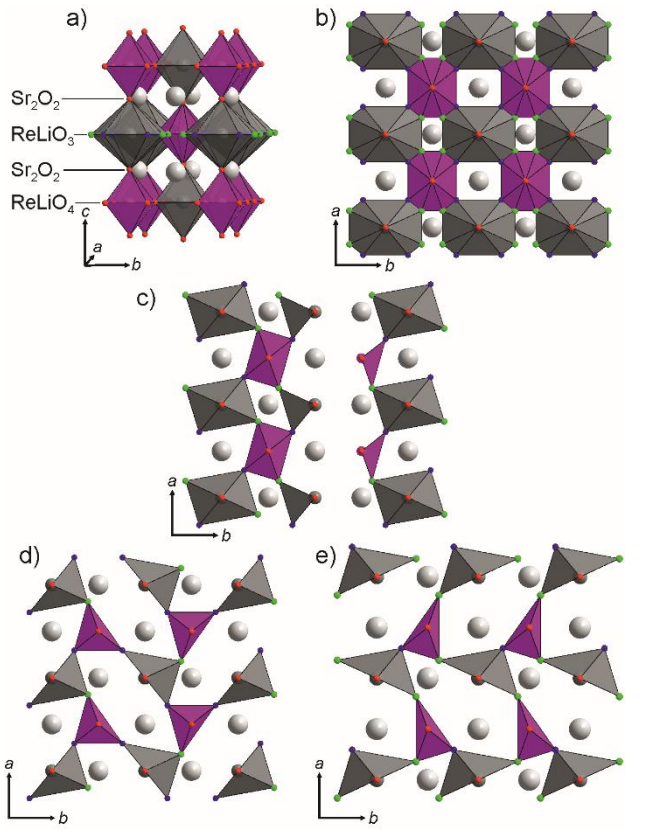

Figure 6. a) The refined structure of $Sr_2ReLiO_{5.5}$ viewed in projection approximately along [100]. b) The anion deficient $ReLiO_3$ layered viewed down [001]. Anion-vacancy ordered arrangements of the $ReLiO_3$ layer with c) 4- and 6-fold coordinate metal cations, d) and e) 5-fold coordinate metal cations. Light grey, dark grey and purple spheres represent Sr, Li and Re cations respectively. Red spheres represent fully occupied anions sites (O(1)-O(3)), blue and green spheres represent partially occupied O(4) and O(5) anion sites respectively.

interesting that lithium appears to be playing this role in the Sr_2ReLiO_{6-x} system – suggesting a range of novel topochemically reduced A_2MLiO_{6-x} (M = 4*d*/5*d* transition metal) phases could be prepared and stabilized in this manner.

Cation coordination polyhedra. The anion deficient structure of $Sr_2ReLiO_{5.5}$ consists of alternating oxygen-stoichiometric $ReLiO_4$ layers and anion-deficient $ReLiO_3$ layers, stacked with Sr_2O_2 sheets, as shown in Figure 6a. Diffraction data show no evidence for long-range order of the anion vacancies within the oxygen-deficient layers, however we can construct locally ordered structures and thus plausible local coordination polyhedra, for the Re and Li cations from the partially occupied oxygen site positions within the oxygen deficient layers.

The $ReLiO_3$ stoichiometry and disposition of the partially occupied oxide ions sites within the anion deficient layers (Figure 6b) gives two plausible coordination possibilities for the rhenium and lithium B-site cations. Either all the B-site cations are 5-coordinate (once the apical anions are considered) as shown in Figures 6d and 6e, or there is a 1:1 ratio of 6- and 4-fold coordinate sites, as shown in Figure 6c. This latter arrangement is reminiscent of the structure of $Ho_{0.2}Sr_{0.8}CoO_{2.75}$.[18] Calculating bond valence sums (BVS) for the B-site cations,[19, 20] we observe values of +7.792 and +5.196 for the 6- and 4-fold coordination rhenium cations respectively in this latter structure. Such a large difference in BVS for the two rhenium coordination sites would imply the average Re^{6+} oxidation state had disproportionated into a Re^{5+}/Re^{7+} combination, which is inconsistent with the EELs data. Thus we can discard structural models of this type, and focus on models with 5-fold coordinations for rhenium and lithium.

It is possible to construct two sets of plausible 5-fold coordination polyhedra for the Re and Li cations which reside on the $ReLiO_3$ anion-deficient layers. The metal cations can either reside within an $M[O(2)]_2[O(4)]_2[O(5)]_1$ coordination which gives BVS values of Re +6.596 and Li +0.764 – an ordered array of these coordinations is shown in Figure 6d. Alternatively $M[O(2)]_2[O(4)]_1[O(5)]_2$ polyhedra can be constructed, which give BVS values of Re +6.398 and Li +0.681 - an ordered array of these coordinations is shown in Figure 6e. The BVS values of the cations in these coordinations compare with the values of Re +6.215 and Li +1.139 calculated for the ReO_6 and LiO_6 polyhedra in the anion stoichiometric layers.

Given that neither neutron or electron diffraction show any evidence for long range anion-vacancy order, we propose that the structure of $Sr_2ReLiO_{5.5}$ consists of a long-range disordered array of these coordinations connected into apex-linked sheets which respect the Re/Li cation order of the parent phase. It is likely that small regions of anion vacancy order such as that shown in Figures 6d and 6e exist (analogous to the anion deficient layers present in $Ca_2Mn_2O_5$),[21] but the lack of long range order means we are unable to probe this since the nanoscale twinning prevents imaging of the short range order.

Composition-structure relations. The reduction of Sr_2ReLiO_6 to $Sr_2ReLiO_{5.5}$ leads to dramatic changes to the cation coordination polyhedra. The $Re(1)O_6$ and $Li(1)O_6$ polyhedra which reside within the 'oxygen stoichiometric' layers of the reduced phase expand in a highly anisotropic manner on reduction. In the case of rhenium, this extends the axial Re-O bond by 7.9%, compared to a much more modest 2.2% expansion of the

equatorial Re-O bonds. This anisotropic expansion changes the tetragonal distortion parameter ($Re\text{-}O_{axial}/Re\text{-}O_{equatorial}$) of the $Re(1)O_6$ unit from -0.92% (compression) to +4.3% (expansion). It is tempting to attribute the anisotropic expansion of this polyhedron to an electronic (Jahn-Teller) distortion associated with the change from d^0 Re^{7+} to d^1 Re^{6+}. However, the expected distortion for a d^1 centre would involve a tetragonal compression, leading to a $(d_{xy})^1(d_{xz}/d_{yz})^0$ electronic configuration, rather than an expansion which does not lift the degeneracy of the electronic configuration, and instead results in a $(d_{xz}/d_{yz})^1(d_{xy})^0$ state. We therefore conclude that the large axial elongation of both the $Re(1)O_6$ and $Li(1)O_6$ units is a crystal packing effect which arises from the need to simultaneously satisfy the coordination 'requirements' of the rhenium cations which are being reduced, and the lithium and strontium cations which are not. Furthermore, as described below, many of the large-scale structural features of $Sr_2ReLiO_{5.5}$ can be attributed to such crystal packing effects.

The optimum lattice configuration of the topochemically reduced phase $Sr_2ReLiO_{5.5}$ will lower the BVS of the rhenium cations, compared to Sr_2ReLiO_6, whilst maintaining the sums of the Sr and Li cations, all while respecting the topochemical constraint that the overall topology of the lattice is retained – an effect which has been seen in other systems.[22] The ordering of anion vacancies into alternate anion-deficient and anion-stoichiometric layers means that, in contrast to Re(2) (located in the anion deficient layers) which lowers its BVS by lowering its coordination number, the BVS value of Re(1) can only be lowered to a value consistent with reduction to Re^{6+} by expanding the Re(1)-O bond lengths. An isotropic lengthening of all the Re(1)-O bonds would lead to an isotropic expansion of the anion lattice which would also lower the BVS of the Sr and Li cations – an undesirable outcome. Thus the observed anisotropic distortion of the $ReLiO_4$ layers appears to be a compromise which lowers the BVS of Re without significantly affecting those of Li and Sr. In the case of lithium, the expansion of the $Li(1)O_6$ unit is mitigated by the off-centring of the lithium cation, which raises the BVS of Li(1) slightly.

As noted above it is possible to construct chemically plausible coordination polyhedra for both the Re(2) and Li(2) cations. However, the disorder present in the anion deficient $LiReO_3$ layers of $Sr_2ReLiO_{5.5}$ limits the analysis of the local Re(2) and Li(2) coordinations. One clear observation which can be made is that the expansion of the Re(2)-O and Li(2)-O bonds on reduction is much more isotropic than the corresponding expansions in the anion stoichiometric, $ReLiO_4$ layers. This indicates that it is the highly anisotropic expansion of this later layer which drives the overall anisotropic expansion of the material on reduction, and thus the large-scale twining of the material.

Structure-property relations. The most striking feature of the magnetic behaviour of $Sr_2ReLiO_{5.5}$ is the exceptionally small susceptibility of the phase (C = 0.0319(3) cm^3 K mol^{-1}). This corresponds to an effective Re moment of μ_{eff} = 0.505 μ_B, which is significantly smaller than the spin-only value of μ_{eff} = 1.73 μ_B expected for a d^1 Re^{6+} centre. An obvious explanation for the small Re moment is spin-orbit coupling, however as noted above the reduction of Sr_2ReLiO_6 to $Sr_2ReLiO_{5.5}$ lowers the local symmetry of the ReO_x centres significantly, which might be expected to quench any orbital contribution to the Re moment.

The degree to which the spin-orbit coupling of rhenium is sensitive to the local symmetry can be estimated by comparing the magnetic behaviour of Ba_2CaReO_6,[3] which adopts a cubic crystal structure, and thus retains O_h symmetry ReO_6 units, with Sr_2CaReO_6 and Sr_2MgReO_6 [23, 24] which adopt monoclinic and tetragonal structures respectively and thus have distorted ReO_6 centres. Table 3 lists the effective rhenium moments of these phases, extracted from high-temperature susceptibility data. While fits of the Curie-Weiss law to data from these phases should be treated with caution due to the large θ values obtained, it is clear however that the strontium phases exhibit moments close to the spin-only expectation (1.73 μ_B), while the barium phase exhibits an effective moment which is significantly smaller indicating that while O_h symmetry $Re^{6+}O_6$ centres do exhibit significant spin-orbit coupling, the modest local distortions present in the ReO_6 centres of the strontium phases appear to be sufficient to almost completely remove these orbital contributions.[3] Table 3 also lists the different Re-O bond lengths of the $A_2M^{2+}Re^{6+}O_6$ phases,[3, 23, 24] and it can be seen by comparison to Table 2 that the ReO_6 centres in the $Sr_2M^{2+}Re^{6+}O_6$ phases are less distorted (closer to O_h symmetry) than the ReO_x units in $Sr_2ReLiO_{5.5}$, leading to the initial expectation that there should not be any orbital contribution to the magnetism in the anion-deficient phase. However, the small moment observed for the Re^{6+} cations in $Sr_2ReLiO_{5.5}$ indicates otherwise and demonstrates that Re^{6+} can exhibit strong spin-orbit effects even when residing in lower-symmetry coordination sites. Close inspection of the $Re(1)O_6$ coordination reveals that this unit has D_{2d} symmetry which retains the degeneracy of the d_{xz} and d_{yz} orbitals enabling an orbital contribution to the moment of this centre to be retained. Likewise some of the possible $Re(2)O_5$ coordinations are very close to C_{4v} symmetry which also retains d_{xz}/d_{yz} degeneracy.

Table 3. Magnetic behaviour and local symmetry of $A_2M^{2+}Re^{6+}O_6$ phases.

	Space Group	μ_{eff} (μ_B)	θ (K)	Re-O bond lengths (Å)	ref
Ba_2CaReO_6	Fm-3m	0.744(2)	-39	2.092(1)	3
Sr_2MgReO_6	I4/m	1.72(9)	-426	1.926(8)/1.901(4)	23
Sr_2CaReO_6	P21/n	1.659(6)	-443	1.899(5)/1.908(4)/ 1.925(5)	24

Considering the magnetic behaviour of all the Re^{6+} containing oxide phases it is clear that the influence of local symmetry on the spin-orbit interaction in Re^{6+} oxides is more complex than initially stated.

A further way in which the magnetic behaviour of $Sr_2ReLiO_{5.5}$ differs qualitatively from that of the $A_2M^{2+}Re^{6+}O_6$ phases is that the anion-deficient phase shows no evidence for magnetic order either in magnetisation data or low temperature (2 K) neutron diffraction data. In contrast Sr_2CaReO_6 and Sr_2MgReO_6 are observed to be spin glasses at low temperature (T_{order} = 50 K and 14 K respectively)[23, 24] while Ba_2CaReO_6 has an antiferromagnetic ground state (T_N = 15 K) and Ba_2MgReO_6 a ferromagnetic ground state (T_c = 18 K).[3, 25] Thus we can see that a combination of a strongly reduced moment and lack of low temperature magnetic order exhibited by $Sr_2ReLiO_{5.5}$ does not fit into the general scheme of magnetic behaviour observed for other Re^{6+} double perovskite phases, suggesting the large number of anion-vacancies and large-scale crystallographic disorder in the phase leads to qualitative changes in the magnetic behaviour.

Conclusions

We have demonstrated that topochemical reduction is an effective method for the preparation of oxide phases containing 5d transition metal cations in paramagnetic oxidation states. The phase formed, $Sr_2ReLiO_{5.5}$ exhibits a partially anion-vacancy ordered structure with extensive microstructural twining which arises to minimize crystallographic strain. The Re^{6+} centres in the phase exhibit significantly reduced local paramagnetic moments, despite their location in reduced symmetry coordination sites, indicating spin-orbit coupling is not quenched by small deviations from local O_h symmetry, contrary to widespread belief.

Conflicts of interest

There are no conflicts to declare.

Acknowledgements

Experiments at the Diamond Light Source were performed as part of the Block Allocation Group award "Oxford Solid State Chemistry BAG to probe composition-structure-property relationships in solids" (EE13284). Experiments at the ISIS pulsed neutron facility were supported by a beam time allocation from the STFC. NH acknowledges funding from the "State Programme on Education of Azerbaijani Youth Abroad in 2007-2015" by the Ministry of Education of Azerbaijan. J.V. and N.G. acknowledge funding through the GOA project "Solarpaint" of the University of Antwerp. The microscope used in this work was partly funded by the Hercules Fund from the Flemish Government.

Notes and references

1. G. Cao and L. DeLong, *Frontiers of 4d- and 5d-Transition Metal Oxides*, 2013.
2. G. Cao, J. Bolivar, S. McCall, J. E. Crow and R. P. Guertin, *Phys. Rev. B*, 1998, **57**, R11039-R11042.
3. K. Yamamura, M. Wakeshima and Y. Hinatsu, *J. Solid State Chem.*, 2006, **179**, 605-612.
4. G. Cao, T. F. Qi, L. Li, J. Terzic, S. J. Yuan, L. E. DeLong, G. Murthy and R. K. Kaul, *Phys. Rev. Lett.*, 2014, **112**, 056402.
5. J. E. Page, C. V. Topping, A. Scrimshire, P. A. Bingham, S. J. Blundell and M. A. Hayward, *Inorg. Chem.*, 2018, **57**, 10303-10311.
6. A. S. Erickson, S. Misra, G. J. Miller, R. R. Gupta, Z. Schlesinger, W. A. Harrison, J. M. Kim and I. R. Fisher, *Phys. Rev. Lett.*, 2007, **99**, 016404.
7. H. J. Xiang and M. H. Whangbo, *Phys. Rev. B*, 2007, **75**, 052407.
8. N. N. Greenwood and A. Earnshaw, *Chemistry of the Elements*, Pergamon Press, Oxford, 1997.
9. T. Aharen, J. E. Greedan, C. A. Bridges, A. A. Aczel, J. Rodriguez, G. MacDougall, G. M. Luke, V. K. Michaelis, S. Kroeker, C. R. Wiebe, H. D. Zhou and L. M. D. Cranswick, *Phys. Rev. B*, 2010, **81**, 064436.
10. K. I. Kobayashi, T. Kimura, Y. Tomioka, H. Sawada, K. Terakura and Y. Tokura, *Phys. Rev. B*, 1999, **59**, 11159-11162.
11. M. A. Hayward, in *Comprehensive Inorganic Chemistry II*, eds. J. Reedijk and K. R. Poeppelmeier, Elsevier, Oxford, 2013, vol. 2, pp. 417-453.
12. M. Bharathy and H. C. Z. Loye, *J. Solid State Chem.*, 2008, **181**, 2789-2795.
13. A. C. Larson and R. B. Von Dreele, Los Alamos National Laboratory Report LAUR 86-748, 2000.
14. M. Retuerto, M. J. Martinez-Lope, M. Garcia-Hernandez, M. T. Fernandez-Diaz and J. A. Alonso, *Eur. J. Inorg. Chem.*, 2008, 588-595.
15. J. Verbeeck and S. Van Aert, *Ultramicroscopy*, 2004, **101**, 207-224.
16. F. Denis Romero, S. J. Burr, J. E. McGrady, D. Gianolio, G. Cibin and M. A. Hayward, *J. Am. Chem. Soc.*, 2013, **135**, 1838-1844.
17. M. A. Hayward and M. J. Rosseinsky, *Chem. Mater.*, 2000, **12**, 2182-2195.
18. M. James, M. Avdeev, P. Barnes, L. Morales, K. Wallwork and R. Withers, *J. Solid State Chem.*, 2007, **180**, 2233-2247.
19. I. D. Brown and D. Altermatt, *Acta Crystallogr., Sect. B : Strucut. Sci.*, 1985, **B41**, 244-247.
20. N. E. Brese and M. O'Keeffee, *Acta Crystallogr., Sect. B : Strucut. Sci.*, 1991, **B47**, 192-197.
21. K. R. Poeppelmeier, M. E. Leonowicz, J. C. Scanlon, J. M. Longo and W. B. Yelon, *J. Solid State Chem.*, 1982, **45**, 71-79.
22. M. A. Hayward, *Semicond. Sci. Technol.*, 2014, **29**, 64010.
23. C. R. Wiebe, J. E. Greedan, P. P. Kyriakou, G. M. Luke, J. S. Gardner, A. Fukaya, I. M. Gat-Malureanu, P. L. Russo, A. T. Savici and Y. J. Uemura, *Phys. Rev. B*, 2003, **68**, 134410.
24. C. R. Wiebe, J. E. Greedan, G. M. Luke and J. S. Gardner, *Phys. Rev. B*, 2002, **65**, 144413.
25. C. A. Marjerrison, C. M. Thompson, G. Sala, D. D. Maharaj, E. Kermarrec, Y. P. Cai, A. M. Hallas, M. N. Wilson, T. J. S. Munsie, G. E. Granroth, R. Flacau, J. E. Greedan, B. D. Gaulin and G. M. Luke, *Inorg. Chem.*, 2016, **55**, 10701-10713.